Check for updates

AGU ADVANCING EARTH AND SPACE SCIENCES

Geophysical Research Letters

RESEARCH LETTER
10.1029/2025GL115227

Does the Dayside Equatorial Ionospheric Electric Field Respond to Isolated Substorms?

M. Hayashi[1], A. Yoshikawa[2,3], and S. Ohtani[4]

[1]Department of Earth and Planetary Sciences, Graduate School of Science, Kyushu University, Fukuoka, Japan, [2]Department of Earth and Planetary Sciences, Faculty of Science, Kyushu University, Fukuoka, Japan, [3]International Research Center for Space and Planetary Environmental Science, Kyushu University, Fukuoka, Japan, [4]Johns Hopkins University Applied Physics Laboratory, Laurel, MD, USA

Key Points:

- Electric field penetration associated with isolated substorms was not statistically significant at the dayside equator
- The dayside equatorial H component tends to decrease after isolated substorm onsets as a remote effect of the substorm current wedge

Supporting Information:

Supporting Information may be found in the online version of this article.

Correspondence to:

M. Hayashi,
hayashi.moe.045@s.kyushu-u.ac.jp

Citation:

Hayashi, M., Yoshikawa, A., & Ohtani, S. (2025). Does the dayside equatorial ionospheric electric field respond to isolated substorms? *Geophysical Research Letters*, *52*, e2025GL115227. https://doi.org/10.1029/2025GL115227

Received 8 FEB 2025
Accepted 3 MAY 2025

Abstract Substorms are known to induce global magnetosphere-ionosphere coupling. However, the specific response of the dayside ionospheric electric field and its influence on the equatorial electrojet (EEJ) remain controversial. This study investigates the electromagnetic field response in the dayside equatorial region during isolated substorms using ground magnetic field data. Statistical analysis revealed that the H component decreased at equatorial and low-latitude stations during isolated substorms. These decreases were of similar magnitude on average, indicating that significant changes in the EEJ caused by penetrating electric fields were not observed. However, individual events showed slight positive and negative variations. These results suggest that substorm-associated electric fields can reach equatorial regions, but additional conditions determine the positive and negative variations. This finding provides new insights into the spatial extent of substorm-induced electric fields.

Plain Language Summary Substorms are disturbances in the Earth's magnetosphere that cause strong electric and magnetic field changes, mainly at high latitudes. While previous studies have discussed how substorm-associated electric fields influence the dayside equatorial ionosphere, a definitive conclusion has yet to be reached. This study analyzed geomagnetic data from low-latitude and equatorial stations to examine electric field penetration during isolated substorms. The results show that, on average, no significant penetration was observed. Instead, changes in the equatorial magnetic field were mainly caused by remote effects from the substorm current wedge rather than electric field penetration. However, small variations in electric fields appeared in individual events, suggesting that weak penetration may still occur under specific conditions. These findings improve our understanding of global magnetosphere-ionosphere coupling, which influences space weather and satellite operations.

1. Introduction

Various current systems are generated and developed during substorms in the high-latitude magnetosphere and ionosphere. In the polar ionosphere, two major current systems evolve: the Region 1 (R1) current at higher latitudes and the Region 2 (R2) current at lower latitudes (Iijima & Potemra, 1976). The R1 current, associated with magnetospheric convection, intensifies during the growth phase of a substorm. In contrast, the R2 current, which flows in the opposite direction to the R1 current, is driven by pressure gradients in the inner magnetosphere and becomes stronger when substorms induce high-pressure plasma in this region (e.g., Jayachandran et al., 2003; Miyashita et al., 2008). In addition to developing these currents, strong plasma injection generates a substorm current wedge (SCW) with the same polarity as the R1 current system at the onset of the substorm (McPherron et al., 1973).

As the R1 and R2 currents develop, they create potentials that drive electric fields in the polar ionosphere, with each current producing electric fields in opposite directions. The imbalance between R1 and R2 currents plays a significant role in electric field responses in the mid, low, and equatorial ionosphere. Observational and simulation-based studies have reported both eastward and westward electric field penetration to the equatorial ionosphere during substorms, depending on the development and interplay of R1 and R2 currents. For example, Huang et al. (2004), Huang (2009), and Fejer and Navarro (2022) reported that an eastward electric field associated with R1 current development dominates the dayside low-latitude ionosphere at substorm onset. Conversely, other studies have observed westward electric fields on the dayside at substorm onset (Gonzales

© 2025. Johns Hopkins University Applied Physics Laboratory and The Author(s). This is an open access article under the terms of the Creative Commons Attribution-NonCommercial License, which permits use, distribution and reproduction in any medium, provided the original work is properly cited and is not used for commercial purposes.

19448007, 2025, 10, Downloaded from https://agupubs.onlinelibrary.wiley.com/doi/10.1029/2025GL115227, Wiley Online Library on [11/08/2025]. See the Terms and Conditions (https://onlinelibrary.wiley.com/terms-and-conditions) on Wiley Online Library for rules of use; OA articles are governed by the applicable Creative Commons License

et al., 1979), accompanied by decreases in the H magnetic component (e.g., Kikuchi et al., 2003; Wei et al., 2009). These observations align with the overshielding electric field generated by the R2 current's development.

Although several studies have investigated the penetration and overshielding electric fields associated with the development and decay of R1 and R2 currents, the statistical characteristics of these phenomena are still not fully understood.

Another key factor influencing magnetic field disturbances during substorms is the SCW. Ohtani et al. (2021) examined global ground magnetic disturbance regarding the SCW. They found that the H component decrease in the dayside equatorial region during substorms was due to remote effects of the SCW. The remote effect of the SCW is a ground magnetic disturbance generated by the field-aligned currents of SCW based on Biot–Savart's law. These findings suggest that the SCW strongly influences dayside magnetic disturbances more than local ionospheric currents. Conversely, the dayside Pi2 pulsations suggest the presence of a global ionospheric current system that connects the SCW to the equatorial electrojet (EEJ) at the substorm onset (Imajo et al., 2015, 2017). However, the temporal evolution of the global current system over substorm timescales (1–2 hr) remains unclear. Although some studies have suggested a relationship between the dayside electromagnetic field response and the SCW, many aspects of this interaction are not fully understood.

As mentioned above, several studies have investigated electromagnetic field responses during substorms. However, two key aspects remain unresolved. First, the statistical characteristics of mid- and low-latitude and equatorial electric field responses during substorms remain unclear. Second, the temporal evolution of the dayside current system connected to the SCW has yet to be fully understood. To advance our understanding of these issues, it is essential to statistically examine the EEJ response in the dayside equatorial region at the onset of substorm. In the present paper, we statistically analyze the electromagnetic field responses during 170 isolated substorms that occurred between 2009 and 2011, focusing on geomagnetic variations at the onset of substorms in the dayside equatorial and low-latitude regions.

Section 2 analyzes the magnetic and electric field disturbances on the dayside with case studies and statistical analysis. Section 3 discusses the results, and Section 4 concludes this study.

2. Results

2.1. Data and Methodology

We identified substorms using the AL index and the nightside positive bay. The AL index was obtained from the (World Data Center for Geomagnetism et al., 2015), Kyoto, Japan, and the positive bay was observed in Paratunka (PTK: magnetic latitude, 46.70°; magnetic longitude, 227.24°; LT = UT + 10.0 hr), Russia. Substorm events were selected based on the following criteria: the AL index remained above −100 nT two hours before the onset and dropped below −200 nT afterward. The threshold of −100 nT is consistent with previous studies of the substorm growth phase (e.g., Gjerloev et al., 2007; Ohtani & Gjerloev, 2020). The −200 nT threshold was determined based on the approach used in Ohtani and Gjerloev (2020), which identifies substorm onset by requiring a decrease of at least 100 nT from the value at the onset. Among these events, we focused on 170 cases where the equatorial station was on the dayside (MLT: 10–14 hr) from 2009 to 2011.

To examine the dayside electromagnetic field response during substorms, we analyzed magnetic field data from two stations: Mbour (MBO: magnetic latitude, 1.20°; magnetic longitude, 58.44°; dip latitude = 3.38; LT = UT–1.3 hr) and Guimar (GUI: magnetic latitude, 16.06°; magnetic longitude, 60.99°; LT = UT–1.16 hr). The variation of the EEJ due to electric field penetration in the equatorial region on the dayside was detected by subtracting the H component at GUI from that at MBO. This approach was based on the theory that the equatorial ionospheric current is enhanced by the Cowling effect (Hirono, 1952), which enhances the response of the equatorial H to externally imposed electric fields. As a result, when an electric field penetrates the equatorial region, the variation in the H component becomes more pronounced at the equator than at low latitudes, allowing the equatorial ionospheric electric field to be inferred from the difference in H components between a station near the geomagnetic equator and another located off the equator (Anderson et al., 2002).

The magnetic field data in PTK is part of the MAGnetic Data Acquisition System/Circum-pan Pacific Magnetometer Network Data (MAGDAS/CPMN) (Yumoto & the MAGDAS Group, 2006, 2007), with details available on the International Center for Space and Planetary Environmental Research (i-SPES). Other ground magnetic

19448007, 2025, 10, Downloaded from https://agupubs.onlinelibrary.wiley.com/doi/10.1029/2025GL115227, Wiley Online Library on [11/08/2025]. See the Terms and Conditions (https://onlinelibrary.wiley.com/terms-and-conditions) on Wiley Online Library for rules of use; OA articles are governed by the applicable Creative Commons License

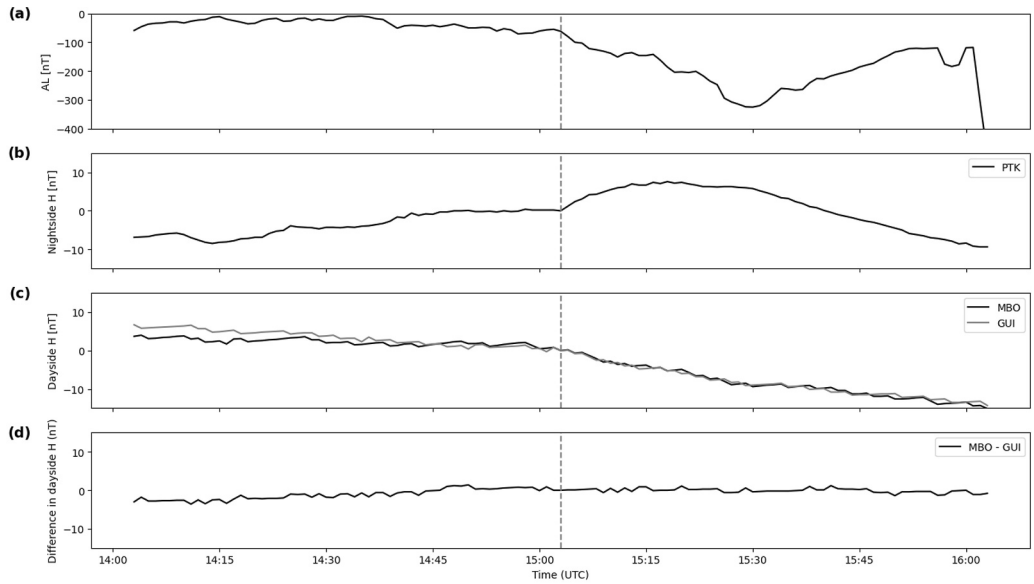

Figure 1. (a) AL index on 23 November 2010. (b) The H component at PTK (LT = UT + 10hr) on the nightside. (c) The H component at MBO (LT = UT + 22.7 hr) and GUI (LT = UT + 22.8 hr). (d) Difference in the H components between MBO and GUI.

field data were provided by the SuperMAG database, which standardizes data from different sources. Specifically, the data for MBO was obtained from the Bureau Central de Magnétisme Terrestre, while the data for GUI was obtained from the Instituto Geográfico Nacional. Geomagnetic field data from MBO and GUI are subtracted for daily variations and yearly trends.

2.2. Global Electromagnetic Field Response–Case Study

In this section, we investigate the response of the dayside electric and magnetic fields during an isolated substorm on 23 November 2010, at 15:03 UT. This event is one of the 170 isolated substorm events selected in Section 2.1. Figures 1a–1e present the following parameters for the ±1 hr interval around the substorm onset: (a) the AL index, (b) the H component at PTK, (c) the H components at MBO and GUI, and (d) the difference in the H components between MBO and GUI. PTK is on the night side, whereas MBO and GUI are on the dayside.

The black vertical dashed line at 15:03 UT indicates the onset of the substorm. The AL index decreased at 15:03 UT, reaching a minimum of −323 nT at 15:30 UT (Figure 1a). Simultaneously, the H component at PTK increased, showing a positive bay that peaks at 15:17 UT (Figure 1b).

On the dayside, the H components at MBO and GUI decreased by similar amplitudes at the onset (Figure 1b). The H components were offset relative to their values at the onset. Since the H components at MBO and GUI decreased with almost the same amplitude, and the difference between the two remained close to zero before and after the onset (Figure 1c), these results suggest that the electric field associated with the substorm did not penetrate the dayside equator and thus did not induce a variation in the EEJ. Instead, the decrease in the dayside H component is likely attributed to the remote effect of the SCW, not to the penetration of the electric field.

2.3. Statistical Analysis of the Dayside Electric and Magnetic Response Using Superposed Epoch Analysis

This section examines the electromagnetic field response in the dayside equatorial region during isolated substorms using statistical methods. Specifically, superposed epoch analysis was applied to investigate variations in the H components at equatorial and low-latitude stations during 170 isolated substorms observed between 2009 and 2011.

Figures 2a–2g illustrate the superposed epoch analysis for the AL index, the H components at MBO and GUI, the difference in the H components between MBO and GUI, and their offset-adjusted values over a ±2.5 hr interval around the substorm onset. The x-axis represents the elapsed time from the substorm onset, with t = 0

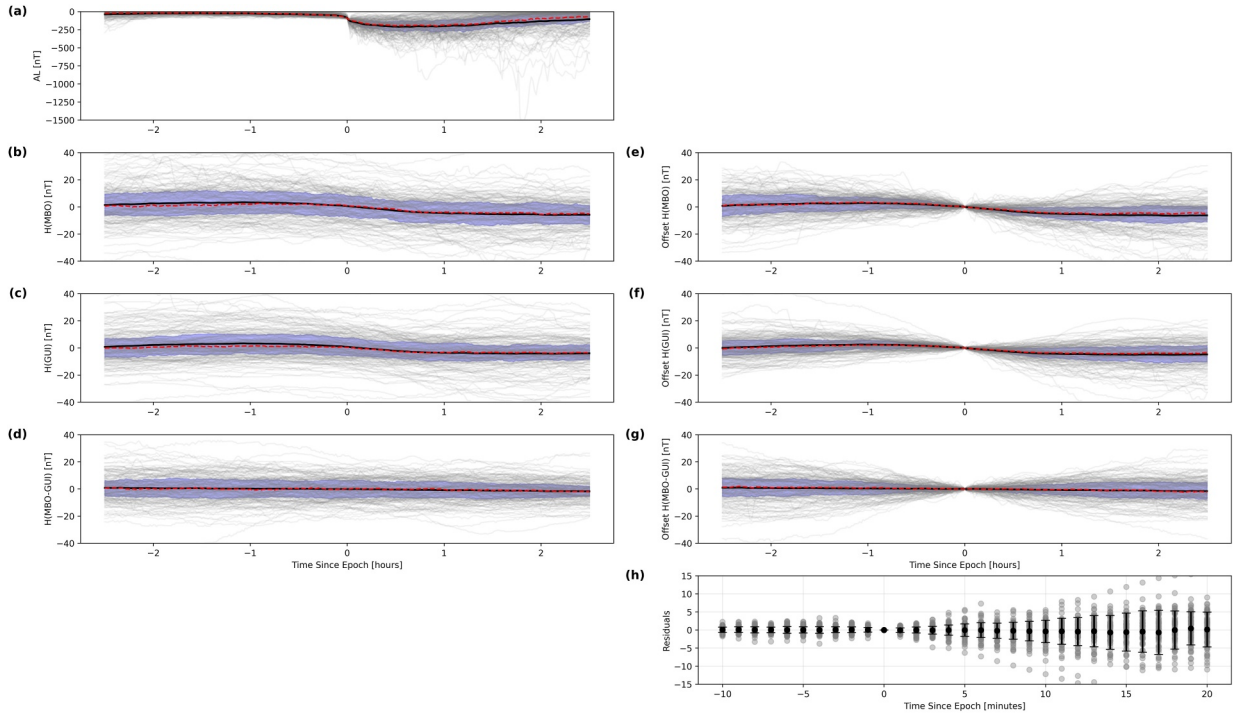

Figure 2. Superposed epoch analysis for 170 isolated substorms. (a) AL index. (b) H component variations at MBO. (c) H component variations at GUI. (d) Difference in H components between MBO and GUI. (e) Offset-adjusted H component magnetic field at MBO (subtracting the value at $t = 0$ for each event). (f) Offset-adjusted H component at GUI, using the same method as in panels (e, g) Offset-adjusted difference in H component between MBO and GUI, where the value at $t = 0$ serves as the offset for each event. The thin lines show the magnetic field variations for each event, and the black solid line, red dotted line, and purple shading indicate the mean, median, and interquartile range of all events. (h) Residuals calculated for the MBO-GUI difference data based on linear regression of 10-min data before zero-epoch.

corresponding to the onset. Thin gray lines show the magnetic field variations for individual events, and the black solid line, red dotted line, and purple shading represent the mean, median, and interquartile range (IQR) of all events, respectively.

At $t = 0$, the AL index decreased, reaching an average drop of 200 nT (Figure 2a). Correspondingly, the H components at MBO and GUI showed gradual decreases in line with the AL index reduction (Figures 2b, 2c, 2e, and 2f). The decrease at MBO and GUI was almost the same, with the difference between the two stations remaining close to zero before and after the onset (Figures 2d and 2g). Furthermore, the mean, median, and IQR of the difference remained steady throughout the analyzed period (Figures 2d and 2g). These findings indicate that, on average, electric field penetration associated with substorms has minimal influence on the dayside equatorial region during isolated substorms. However, as shown in Figure 2g, while the average difference between MBO and GUI is approximately zero, individual events exhibit variability after the onset.

To examine whether the ΔH variations (the difference in H components between equatorial and low-latitude stations) after substorm onset were influenced by pre-existing trends or were newly induced by substorm activity, we conducted a more detailed analysis. Temporal changes in ΔH and the AL 10 min before substorm onset were used to construct a linear regression model, which was then used to extrapolate ΔH values for the 20 min following the onset. The extrapolated values were compared with the observed ΔH values, and residuals (differences between extrapolated and observed values) are shown in Figure 2h. The residuals were calculated as:

$$\Delta H_{\mathrm{res}}(t) = \Delta H_{\mathrm{obs}}(t) - \Delta H_{\mathrm{pred}}(t)$$

where $\Delta H_{\mathrm{obs}}(t)$ represents the observed ΔH at time t, and $\Delta H_{\mathrm{pred}}(t)$ is the predicted value obtained from the linear regression model:

$$\Delta H_{\mathrm{pred}}(t) = \Delta H_0 - m \cdot t$$

19448007, 2025, 10, Downloaded from https://agupubs.onlinelibrary.wiley.com/doi/10.1029/2025GL115227, Wiley Online Library on [11/08/2025]. See the Terms and Conditions (https://onlinelibrary.wiley.com/terms-and-conditions) on Wiley Online Library for rules of use; OA articles are governed by the applicable Creative Commons License

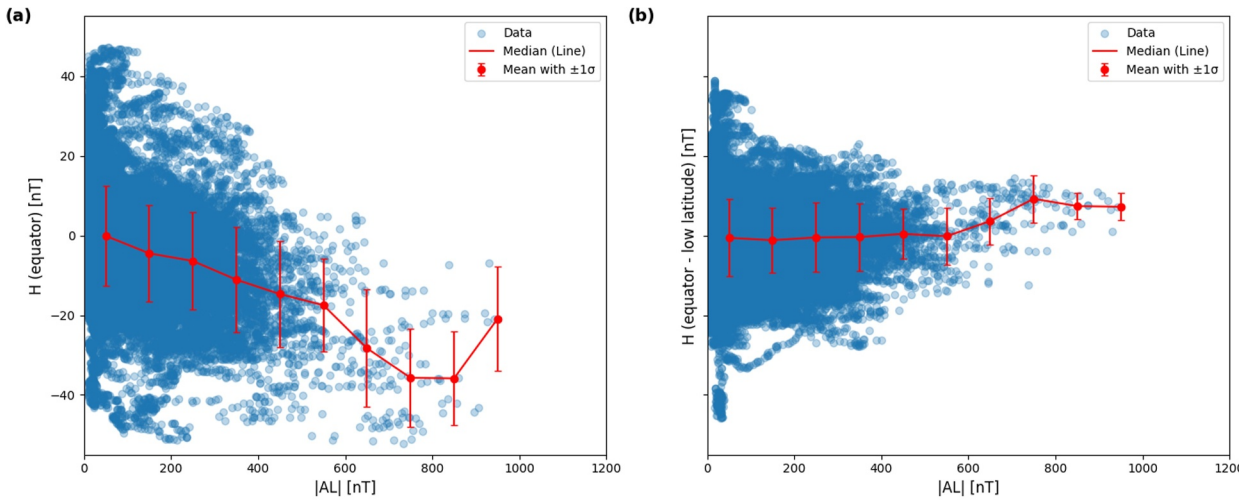

Figure 3. (a) AL index dependence of the H component response at the dayside equator. (b) AL index dependence of the electric field response at the dayside equator, represented by ΔH (the difference in H components between equatorial and low-latitude stations).

where ΔH_0 is the observed ΔH at onset ($t = 0$), and m is the slope obtained from the pre-onset trend ($-10 \leq t < 0$). In Figure 2h, the error bars represent the mean and standard deviation of the residuals. As shown in Figure 2h, variations in ΔH remain close to zero before the onset ($T < 0$), indicating that pre-existing trends were effectively removed. This suggests that the pre-onset trend can be reliably extrapolated for comparison with post-onset variations. After the onset, these residuals showed both positive and negative values, with their standard deviation increasing over time. This indicates that while electric fields associated with substorms may penetrate the equatorial region, their effects are determined by additional conditions that cause the variations to become positive or negative, ultimately canceling each other out on average.

Next, we examined how the scale of the substorm affects the dayside electromagnetic field response. As shown in Figure 3a, we compared the AL index from Figure 2a with the equatorial H component from Figure 2b. The x-axis represents the absolute value of the AL index, with red dots indicating the median value within each 100 nT interval and error bars representing ±1σ. The results that larger AL index values are associated with more significant decreases in the equatorial H component.

There are two possible explanations for this decrease. First, larger substorms may lead to stronger SCW development, amplifying its remote effects. Second, larger substorms may induce a dusk-to-dawn electric field penetration that reduces the H component. To distinguish between these possibilities, we further examined the relationship between the AL index and the electric field response. Figure 3b shows all data points for the AL index from Figure 2a and ΔH from Figure 2c. Figure 3b shows that the ΔH does not vary significantly with increasing AL index values. This suggests that the decrease in the equatorial H component on the dayside is predominantly caused by the remote effects of the SCW, rather than by direct electric field penetration.

Interestingly, when the AL index exceeds 600 nT, the equatorial H component decreases more significantly (Figure 3a). However, ΔH increases positively (Figure 3b). The positive ΔH corresponds to a dawn-to-dusk electric field. Therefore, the pronounced decrease in the equatorial H component for AL values above 600 nT is likely due to factors other than electric field penetration. Further investigation of this phenomenon is beyond the scope of this study.

2.4. Effects of Substorm and IMF Bz on Dayside Electromagnetic Field Response

We investigated the potential influence of the interplanetary magnetic field (IMF) Bz on the dayside electromagnetic field response. Previous studies have suggested that westward electric field disturbances and decreases in the H component observed on the dayside could result from the northward turning of IMF Bz, rather than substorm activity itself (Huang, 2009). To evaluate this possibility, we performed a superposed epoch analysis of IMF Bz.

19448007, 2025, 10, Downloaded from https://agupubs.onlinelibrary.wiley.com/doi/10.1029/2025GL115227, Wiley Online Library on [11/08/2025]. See the Terms and Conditions (https://onlinelibrary.wiley.com/terms-and-conditions) on Wiley Online Library for rules of use; OA articles are governed by the applicable Creative Commons License

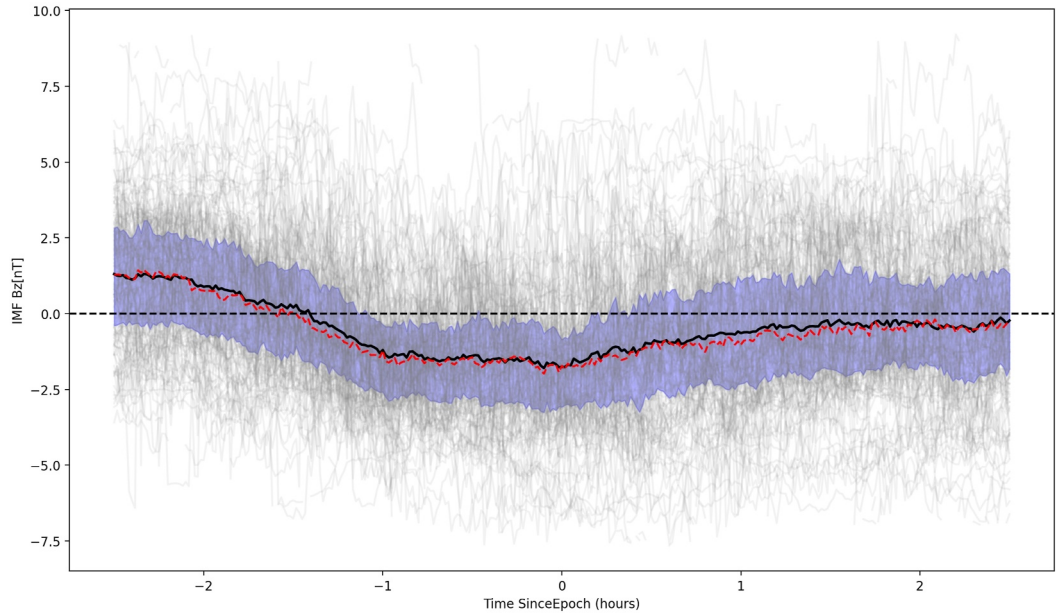

Figure 4. Superposed epoch analysis of interplanetary magnetic field Bz for 170 isolated substorms in the same format as Figure 2.

Figure 4 presents the superposed epoch analysis results for IMF Bz, using the same set of events selected in Section 2.1. On average, IMF Bz turned southward approximately 1.5 hr before onset, reached a minimum of around −2 nT at onset, and exhibited a slight decrease in its southward intensity after the onset. This reduction in the southward IMF Bz may partially contribute to the decrease in the dayside H component (Fejer, 1986).

To further quantify and differentiate the contributions of substorm activity (represented by the AL index) and IMF Bz to the dayside electromagnetic field response, we conducted a multiple regression analysis. This approach enabled us to assess the individual effects of these two factors on both dayside magnetic field disturbances and electric field responses.

The analysis revealed that the AL index had a significantly larger impact on the dayside equatorial H component compared to IMF Bz. Specifically, for every 100 nT decrease in the AL index, the H component decreased by approximately 4.04 nT. In contrast, 1 nT decrease in IMF Bz corresponded to only a 0.0655 nT reduction in the H component. The statistical significance of the AL index was highly robust ($p < 0.0001$), indicating that substorm activity is the primary driver of the observed decrease in the H component at the dayside equatorial region. Although IMF Bz also exhibited statistical significance ($p = 0.003$), its overall effect was relatively minor.

We also evaluated the influence of the AL index and IMF Bz on electric field penetration, as represented by ΔH. The multiple regression analysis showed that neither variable effectively explained variations in electric field penetration, as indicated by the very low R-squared value (R-squared = 0.001). While the AL index was statistically significant ($p < 0.0001$), its effect was minimal, with a 100 nT decrease in the AL index resulting in only a 0.26 nT reduction in ΔH. Furthermore, IMF Bz had no statistically significant impact on electric field penetration ($p = 0.719$).

To provide additional clarity, partial regression plots illustrating the relationships between the AL index, IMF Bz, and the dependent variables (dayside equatorial H component and electric field penetration) are included in Supporting Information S1. These plots visually demonstrate the unique contributions of each independent variable after accounting for the influence of the other.

These results underscore that substorm activity, rather than variations in IMF Bz, primarily drives the reduction in the dayside equatorial H component.

19448007, 2025, 10, Downloaded from https://agupubs.onlinelibrary.wiley.com/doi/10.1029/2025GL115227, Wiley Online Library on [11/08/2025]. See the Terms and Conditions (https://onlinelibrary.wiley.com/terms-and-conditions) on Wiley Online Library for rules of use; OA articles are governed by the applicable Creative Commons License

19448007, 2025, 10, Downloaded from https://agupubs.onlinelibrary.wiley.com/doi/10.1029/2025GL115227, Wiley Online Library on [11/08/2025]. See the Terms and Conditions (https://onlinelibrary.wiley.com/terms-and-conditions) on Wiley Online Library for rules of use; OA articles are governed by the applicable Creative Commons License

3. Discussion

This study statistically investigated the electromagnetic field response on the dayside during isolated substorms using ground magnetic field data. We found that on average, the H components at equatorial and low-latitude stations decreased by similar amplitudes, with the differences between them remaining close to zero before and after substorm onset (Figure 2). These results suggest that, on average, electric field penetration associated with the substorm was not observed on the dayside during isolated substorms.

Although our results showed a decrease in the H component on the dayside, previous studies, such as Clauer et al. (2006) and Huang (2009), reported an increase during substorms. A key difference is that these studies focused on sawtooth events during geomagnetic storms. Moreover, the substorms they analyzed coincided with a strongly southward IMF Bz, suggesting that the reported H component increases were likely driven by strong magnetospheric convection rather than substorm activity alone.

Most previous studies have shown that the dayside equatorial response is typically characterized by H component decrease (e.g., Clauer & McPherron, 1974), consistent with our findings. However, these studies also noted westward electric field disturbances (e.g., Gonzales et al., 1979; Kikuchi et al., 2003; Sastri et al., 2003; Sibeck et al., 1998). It has been proposed that the westward electric field and the negative bay could result from the northward turning of IMF Bz rather than the substorm itself (Huang, 2009). Indeed, many substorm onsets analyzed in these studies were associated with a northward turning of IMF Bz. As shown in Section 2.4, the statistical contribution of the AL index to the reduction of the H component in the dayside equatorial region was far more significant than that of IMF Bz. This result indicates that the H component decrease during substorm is primarily driven by substorm activity rather than IMF Bz variations. Furthermore, the dependence of the H component decrease on the AL index suggests that larger substorms produce stronger magnetic field disturbances in the dayside equatorial region. However, the difference in H components between equatorial and low-latitude stations did not exhibit a clear AL dependence, indicating that direct electric field penetration is not the primary driver of these variations. Instead, the observed decrease in the equatorial H component is predominantly attributed to the remote effects of the SCW, which intensifies with increasing substorm strength.

Previous research has reported that substorms can alter the dayside equatorial H component by tens to hundreds of nT (Hashimoto et al., 2011, 2017; Huang, 2009). Studies comparing low-latitude and equatorial H component variations have noted that equatorial amplitudes are often 2.5 times larger than those at low latitudes (Kikuchi et al., 2000) and can be two to three times larger during geomagnetic storms (Huang et al., 2004; Wei et al., 2009). In our study, the equatorial H component decreased by approximately 4.04 nT for every 100 nT reduction in the AL index (Section 2.4), consistent with previous findings. However, ΔH decreased by only 0.0655 nT for each 100 nT decrease in the AL index (Section 2.4). This suggests that, on average, electric field penetration was not observed on the dayside equator. However, as shown in Figure 2h, individual events exhibit small changes in ΔH after onset, suggesting that weak electric field penetration may still occur. The fact that this variation does not show a consistent polarity suggests that additional factors influence whether the electric field becomes positive or negative. One possible factor is the combined effect of IMF Bz and substorm activity. Our analysis showed that, on average, the substorms examined in this study were accompanied by a northward turning of IMF Bz. However, some events exhibited southward turning or remained relatively steady. This variability in IMF Bz conditions may play a role in modulating the direction of the penetrating electric field, leading to both positive and negative variations. Future studies should classify events based on IMF Bz variations to determine how these different conditions influence the equatorial response. The weak electric field penetration during isolated substorms is likely influenced by how the current system closes. If the substorm current system primarily closes on the nightside, its extension to the dayside could be restricted, limiting the penetration of the associated electric fields. This is in contrast to substorms occurring during magnetic storms, where stronger disturbances may allow for more significant electric field penetration. Since the equatorial response may depend on the latitude and regional characteristics of the observation station, caution is required when directly comparing the magnitude of H component variations due to electric field penetration with previous studies.

Our findings also raise questions about the absence of equatorial enhancement during substorms, contrasting with earlier reports of Pi2 enhancements at substorm onset (e.g., Sastry et al., 1983). These enhancements have been interpreted as evidence of a global current system connecting the SCW through the terminator to the dayside equatorial region (Imajo et al., 2015). Further studies are needed to determine whether equatorial enhancements or

19448007, 2025, 10, Downloaded from https://agupubs.onlinelibrary.wiley.com/doi/10.1029/2025GL115227, Wiley Online Library on [11/08/2025]. See the Terms and Conditions (https://onlinelibrary.wiley.com/terms-and-conditions) on Wiley Online Library for rules of use; OA articles are governed by the applicable Creative Commons License

global current systems extending to the dayside equatorial region are transient phenomena restricted to the onset of substorms or are specific to certain frequency ranges.

4. Conclusions

Our results showed that the H components at equatorial and low-latitude stations decreased by similar amplitudes, and their difference remained statistically insignificant throughout the substorm on average. This suggests that electric field penetration into the dayside equatorial region is generally limited, contrasting with previous reports of significant ΔH variations attributed to penetrating or overshielding electric fields. However, individual events exhibited small deviations in ΔH variations, implying that substorm-associated electric fields may reach the equatorial region but are determined by additional factors, leading to positive and negative variations that cancel out on average.

Furthermore, our analysis revealed that the equatorial H component decrease exhibits a clear dependence on substorm intensity, as indicated by the AL index. Larger substorms tend to produce stronger reductions in the equatorial H component, likely due to enhanced SCW development and its associated remote effects. However, the difference in H components between equatorial and low-latitude stations did not show a significant AL dependence, suggesting that direct electric field penetration does not systematically increase with substorm intensity. These findings emphasize that the primary driver of the observed magnetic field variations is the remote effect of the SCW rather than the direct penetration of substorm-associated electric fields.

The statistical analysis further demonstrated that the decrease in the dayside H component was more strongly correlated with the AL index than with IMF Bz variations. This suggests that substorm activity, rather than IMF Bz, primarily drives the observed H component decrease.

These findings refine our understanding of substorm-induced electromagnetic field variations and raise further questions regarding the role of global current systems and electric field penetrations. Future investigations should explore the conditions under which these processes become significant, such as their dependence on magnetospheric conditions and the combined effects of IMF Bz and substorm activity.

Data Availability Statement

The AL index was obtained from the World Data Center for Geomagnetism, Kyoto (https://wdc.kugi.kyoto-u.ac.jp/ae_provisional/index.html). Solar wind data were provided by the OMNIWeb service of the Space Physics Data Facility at NASA's Goddard Space Flight Center (https://omniweb.gsfc.nasa.gov/form/omni_min_def.html). Ground magnetic field data from MBO and GUI were sourced from the SuperMAG database (https://supermag.jhuapl.edu/), which includes data from contributors such as the Bureau Central de Magnetisme Terrestre (http://www.bcmt.fr/) and the Instituto Geográfico Nacional (https://www.ign.es/). The data can be downloaded by selecting the "Download Data" tab, specifying the time interval, and choosing the "Subtract Baseline" option. The magnetic field data from PTK were obtained from the MAGnetic Data Acquisition System/Circum-pan Pacific Magnetometer Network (MAGDAS/CPMN) (http://magdas2.i-spes.kyushu-u.ac.jp/). The data are not openly accessible through a public repository, but researchers can request access by submitting a data usage form available at http://magdas2.serc.kyushu-u.ac.jp/datausage/index.html.

Acknowledgments
The AL index was obtained from the World Data Center for Geomagnetism, Kyoto (https://wdc.kugi.kyoto-u.ac.jp/wdc/Sec3.html) (World Data Center for Geomagnetism et al., 2015). Solar wind data were provided by the OMNIWeb service of the Space Physics Data Facility at NASA's Goddard Space Flight Center (http://omniweb.gsfc.nasa.gov/). Ground magnetic field data were sourced from the SuperMAG database (https://supermag.jhuapl.edu/), which standardizes data collected from collaborators, including the Bureau Central de Magnetisme Terrestre (http://www.bcmt.fr/) and the Instituto Geográfico Nacional (https://www.ign.es/). We acknowledge the use of SuperMAG data and express our gratitude to all SuperMAG collaborators (J. W. Gjerloev, 2012). The magnetic field data from PTK were provided by the MAGnetic Data Acquisition System/Circum-pan Pacific Magnetometer Network (MAGDAS/CPMN) (Yumoto & the MAGDAS Group, 2006, 2007), with additional details available through the International Center for Space and Planetary Environmental Research (i-SPES) (http://magdas2.serc.kyushu-u.ac.jp/datausage/index.html). MAGDAS/CPMN observations were supported by the Japan Society for the Promotion of Science (JSPS) Grant-in-Aid for Overseas Scientific Survey and for Publication of Scientific Research Results. This work was supported by the JSPS Grant-in-Aid for JSPS Fellows, Grants 22KJ2480, 20H01961, 21H04518, 22K21345, and 22K03707, National Aeronautics and Space Administration Grant 80NSSC21K0036, and National Science Foundation Grant 2224986.

References

Anderson, D., Anghel, A., Yumoto, K., Ishitsuka, M., & Kudeki, E. (2002). Estimating daytime vertical E×B drift velocities in the equatorial F-region using ground-based magnetometer observations. *Geophysical Research Letters*, *29*(12), 1596. https://doi.org/10.1029/2001GL014562

Clauer, C. R., Cai, X., Welling, D., DeJong, A., & Henderson, M. G. (2006). Characterizing the 18 April 2002 storm-time sawtooth events using ground magnetic data. *Journal of Geophysical Research*, *111*(A4), A04S90. https://doi.org/10.1029/2005JA011099

Clauer, C. R., & McPherron, R. L. (1974). Mapping the local time-universal time development of magnetospheric substorms using mid-latitude magnetic observations. *Journal of Geophysical Research*, *79*(19), 2811–2820. https://doi.org/10.1029/JA079i019p02811

Fejer, B. G. (1986). Equatorial ionospheric electric fields associated with magnetospheric disturbances. In Y. Kamide & J. A. Slavin (Eds.), *Proceedings of chapman conference on solar wind-magnetosphere coupling* (pp. 519–545). Terra Sci.

Fejer, B. G., & Navarro, L. A. (2022). First observations of equatorial ionospheric electric fields driven by storm-time rapidly recurrent magnetospheric substorms. *Journal of Geophysical Research: Space Physics*, *127*(12), e2022JA030940. https://doi.org/10.1029/2022JA030940

Gjerloev, J. W. (2012). The SuperMAG data processing technique. *Journal of Geophysical Research*, *117*(A9), A09213. https://doi.org/10.1029/2012JA017683

Gjerloev, J. W., Hoffman, R. A., Sigwarth, J. B., & Frank, L. A. (2007). Statistical description of the bulge-type auroral substorm in the far ultraviolet. *Journal of Geophysical Research*, *112*(A7), A07213. https://doi.org/10.1029/2006JA012189

Gonzales, C. A., Kelley, M. C., Fejer, B. G., Vickrey, J. F., & Woodman, R. F. (1979). Equatorial electric fields during magnetically disturbed conditions 2. Implications of simultaneous auroral and equatorial measurements. *Journal of Geophysical Research*, *84*(A10), 5803–5812. https://doi.org/10.1029/JA084iA10p05803

Hashimoto, K. K., Kikuchi, T., Tomizawa, I., & Nagatsuma, T. (2017). Substorm overshielding electric field at low latitude on the nightside as observed by the HF Doppler sounder and magnetometers. *Journal of Geophysical Research: Space Physics*, *122*(10), 10851–10863. https://doi.org/10.1002/2017JA024329

Hashimoto, K. K., Kikuchi, T., Watari, S., & Abdu, M. A. (2011). Polar-equatorial ionospheric currents driven by the region 2 field aligned currents at the onset of substorms. *Journal of Geophysical Research*, *116*(A9), A09217. https://doi.org/10.1029/2011JA016442

Hirono, M. (1952). A theory of diurnal magnetic variations in equatorial regions and conductivity of the ionosphere E region. *Journal of Geomagnetism and Geoelectricity Kyoto*, *4*(1), 7–21. https://doi.org/10.5636/jgg.4.7

Huang, C.-S. (2009). Eastward electric field enhancement and geomagnetic positive bay in the dayside low-latitude ionosphere caused by magnetospheric substorms during sawtooth events. *Geophysical Research Letters*, *36*(18). https://doi.org/10.1029/2009GL040287

Huang, C.-S., Foster, J. C., Goncharenko, L. P., Reeves, G. D., Chau, J. L., Yumoto, K., & Kitamura, K. (2004). Variations of low-latitude geomagnetic fields and Dst index caused by magnetospheric substorms. *Journal of Geophysical Research*, *109*(A05219). https://doi.org/10.1029/2003JA010334

Iijima, T., & Potemra, T. A. (1976). Field-aligned currents in the dayside cusp observed by Triad. *Journal of Geophysical Research*, *81*(34), 5971–5979. https://doi.org/10.1029/JA081i034p05971

Imajo, S., Yoshikawa, A., Uozumi, T., Ohtani, S., Nakamizo, A., & Chi, P. J. (2017). Application of a global magnetospheric-ionospheric current model for dayside and terminator Pi2 pulsations. *Journal of Geophysical Research: Space Physics*, *122*(8), 8589–8603. https://doi.org/10.1002/2017JA024246

Imajo, S., Yoshikawa, A., Uozumi, T., Ohtani, S., Nakamizo, A., Marshall, R., et al. (2015). Pi2 pulsations observed around the dawn terminator. *Journal of Geophysical Research: Space Physics*, *120*(3), 2088–2098. https://doi.org/10.1002/2013JA019691

Jayachandran, P. T., MacDougall, J. W., Donovan, E. F., Ruohoniemi, J. M., Liou, K., Moorcroft, D. R., & St-Maurice, J.-P. (2003). Substorm associated changes in the high-latitude ionospheric convection. *Geophysical Research Letters*, *30*(20), 2064. https://doi.org/10.1029/2003GL017497

Kikuchi, T., Hashimoto, K. K., Kitamura, T.-I., Tachihara, H., & Fejer, B. (2003). Equatorial counterelectrojets during substorms. *Journal of Geophysical Research*, *108*(A11), 140. https://doi.org/10.1029/2003JA009915

Kikuchi, T., Lühr, H., Schlegel, K., Tachihara, H., Shinohara, M., & Kitamura, T.-I. (2000). Penetration of auroral electric fields to the equator during a substorm. *Journal of Geophysical Research*, *105*(A10), 23251–23261. https://doi.org/10.1029/2000JA900016

McPherron, R. L., Russell, C. T., & Aubry, M. P. (1973). Satellite studies of magnetospheric substorms on August 15, 1968: 9. Phenomenological model for substorms. *Journal of Geophysical Research*, *78*(16), 3131–3149. https://doi.org/10.1029/JA078i016p03131

Miyashita, Y., Hosokawa, K., Hori, T., Kamide, Y., Yukimatu, A. S., Fujimoto, M., et al. (2008). Response of large-scale ionospheric convection to substorm expansion onsets: A case study. *Journal of Geophysical Research*, *113*(A12). https://doi.org/10.1029/2008JA013586

Ohtani, S., & Gjerloev, J. W. (2020). Is the substorm current wedge an ensemble of wedgelets?: Revisit to midlatitude positive bays. *Journal of Geophysical Research: Space Physics*, *125*(9), e2020JA027902. https://doi.org/10.1029/2020JA027902

Ohtani, S., Imajo, S., Nakamizo, A., & Gjerloev, J. W. (2021). Globally correlated ground magnetic disturbances during substorms. *Journal of Geophysical Research: Space Physics*, *126*(4), e2020JA028599. https://doi.org/10.1029/2020JA028599

Sastri, J. H., Kamide, Y., & Yumoto, K. (2003). Signatures for magnetospheric substorms in the geomagnetic field of dayside equatorial region: Origin of the ionospheric component. *Journal of Geophysical Research*, *108*(A10), 1375. https://doi.org/10.1029/2003JA009962

Sastry, T. S., Sarma, Y. S., Sarma, S. V. S., & Narayan, P. V. S. (1983). Day-time Pi pulsations at equatorial latitudes. *Journal of Atmospheric and Terrestrial Physics*, *45*(11), 733–741. https://doi.org/10.1016/s0021-9169(22)00001-0

Sibeck, D. G., Takahashi, K., Yumoto, K., & Reeves, G. D. (1998). Concerning the origin of signatures in dayside equatorial ground magnetograms. *Journal of Geophysical Research*, *103*(A4), 6763–6769. https://doi.org/10.1029/97JA03600

Wei, Y., Pu, Z., Hong, M., Zong, Q., Ren, Z., Fu, S., et al. (2009). Westward ionospheric electric field perturbations on the dayside associated with substorm processes. *Journal of Geophysical Research*, *114*(A12), A12209. https://doi.org/10.1029/2009JA014445

World Data Center for Geomagnetism, Kyoto, M. N., Iyemori, T., Sugiura, M., & Kamei, T. (2015). Geomagnetic AE index. https://doi.org/10.17593/15031-54800

Yumoto, K., & the MAGDAS Group (2006). MAGDAS project and its application for space weather. In *Solar influence on the heliosphere and Earth's environment: Recent progress and prospects* (pp. 309–405). N. Gopalswamy & A. Bhattacharyya (Eds.). ISBN-81-87099-40-2

Yumoto, K., & the MAGDAS Group. (2007). Space weather activities at SERC for IHY: MAGDAS. *Bulletin of the Astronomical Society of India*, *35*, 511–522.

19448007, 2025, 10, Downloaded from https://agupubs.onlinelibrary.wiley.com/doi/10.1029/2025GL115227, Wiley Online Library on [11/08/2025]. See the Terms and Conditions (https://onlinelibrary.wiley.com/terms-and-conditions) on Wiley Online Library for rules of use; OA articles are governed by the applicable Creative Commons License